JOURNAL OF
AGRICULTURAL AND FOOD CHEMISTRY

A Comparative Study of the Antioxidant Power of Flavonoid Catechin and Its Planar Analogue

MONICA LEOPOLDINI, NINO RUSSO,* AND MARIROSA TOSCANO

Dipartimento di Chimica and Centro di Calcolo ad Alte Prestazioni per Elaborazioni Parallele e
Distribuite-Centro d'Eccellenza MIUR, Universita' della Calabria,
I-87030 Arcavacata di Rende (CS), Italy

The antioxidant ability of the flavanol catechin and its planar derivative, catechin 1 (PC1), was explored using the DF/B3LYP theoretical approach. Their potentiality in the hydrogen abstraction and electron transfer reactions, the main working mechanisms of antioxidants, was evaluated by computing the values of two key parameters, which are the OH bond dissociation energy and the ionization potential. Results indicated that the effect of a planar arrangement in the catechin molecule is small in the case of the hydrogen abstraction but greater for the electron transfer, since the in vacuo ionization potential value decreases by about 3 kcal/mol. The reaction of these molecules with the hydroperoxyl radical •OOH indicated that the H• abstraction is faster with the planar catechin.

KEYWORDS: Density functional; antioxidants; catechin; BDE

INTRODUCTION

Flavonoids are a group of naturally occurring polyphenolic compounds found in vegetables, fruits, and cereals. They are produced by plants in which they perform a lot of positive actions such as protection from UV light, attraction for pollination and ovoposition, signaling for N-fixation bacteria, and antimicrobical and antiviral activities (*1*).

During the last decades, flavonoids have received growing interest since many epidemiological and biochemical studies have demonstrated that they possess beneficial effects on human health. The main properties are inhibition of tyrosine kinases (*2*) and cAMP phosphodiesterase (*3*), induction of phase II-metabolizing enzymes (*4*), control of cellular growth (*5*), destruction of pathogen organisms (fungi and viruses) (*6*), and inhibition of human immunodeficiency virus (HIV) transcriptase and HIV replication (*7*). Many of these properties are related to their antioxidant activity or, in other words, to their ability to scavenge free radicals and to synergistic effects with physiological antioxidants like glutathione and α-tocopherol and with several enzymes. Free radicals can damage biomolecules (proteins, membrane lipids, and nucleic acids); thus, they are involved in several diseases and aging itself (*8, 9*).

The harmful action of free radicals can be alleviated by antioxidants through two main mechanisms that are reported in the literature (*10–13*) as H-atom or electron transfer reactions. A free radical R• can remove a hydrogen atom or an electron from the antioxidant (ArOH), giving rise to the ArO• and ArOH•+ species whose stability prevents or slows down the chain radical reactions (*10–13*). In this situation, the antioxidant

activity evaluation can be based on the estimation of OH bond dissociation (BDE) and ionization (IP) energy values (*10–13*).

Most of flavonoids are believed to act through the H-atom transfer since higher energies are involved in the one-electron transfer process (*10*). However, when the IP values drop a lot, as in tocopherols and aminophenols (*10*), electron transfer or a concerted charge transfer–proton transfer mechanism may also be possible.

Catechin is a representative member of the flavonoid class, mainly found in green and black teas and in red wines (*14*). It belongs to the flavanols subclass in which the epicatechin, epigallocatechin, epicatechin gallate, and epigallocatechin gallate are also present.

Its structure is made up by two aromatic rings, A and B, connected through the saturated six member ring C (1 in **Scheme 1**). Hydroxylation occurs at the 3′- and 4′-, at the 3-, and at the 5- and 7-positions, in rings B, C, and A, respectively. Electronic delocalization between the two aromatic rings is blocked by the presence of the chromane moiety (ring C).

Recently, some planar analogues of catechin (PCn) were obtained by the reaction of catechin with various ketones having alkyl chains of different lengths (*15*). The evaluation of PCn

Scheme 1. Structure of Catechin and Planar Catechin 1 (PC1)

Antioxidant Power of Flavonoid Catechin

J. Agric. Food Chem., Vol. 55, No. 19, 2007 **7945**
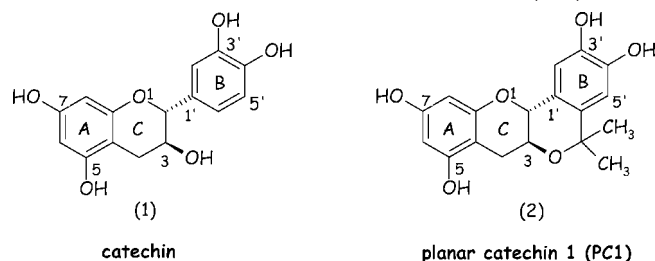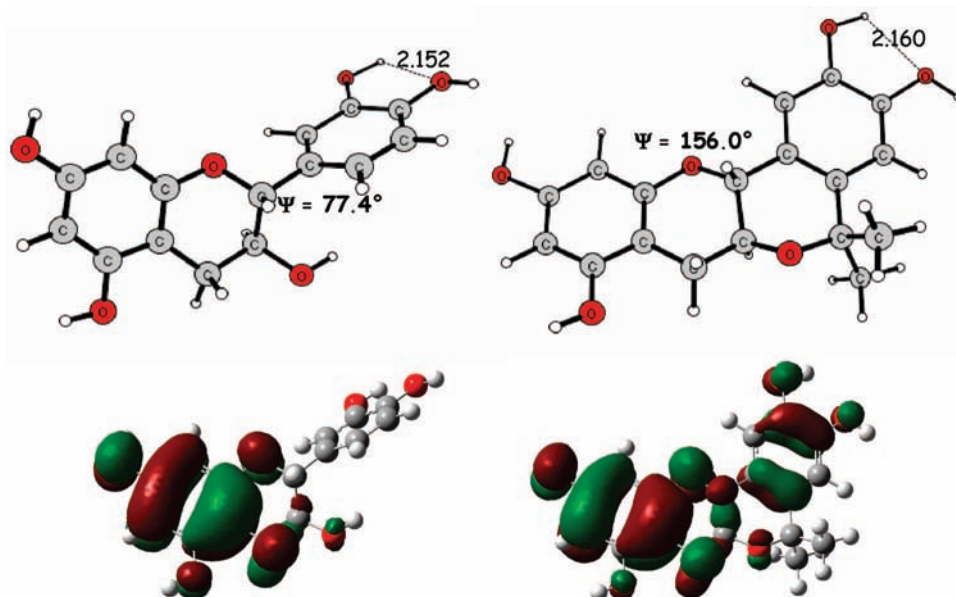
Figure 1. Optimized geometries of catechin (left) and PC1 (right). On the bottom, the HOMOs of both molecules are reported.

radical scavenging activities against the DPPH radical indicated that the hydrogen abstraction in planar catechins is easier than in catechin because of their geometrical configuration. The radical scavenging power of catechin and its planar analogue PC1 (2 in **Scheme 1**) in deaerated MeCN was determined using the galvinoxyl radical (G$^\bullet$) as an oxyl radical species (*16*). Experimental results indicated that the second-order rate constant k values for hydrogen abstraction from catechin and PC1 by G$^\bullet$ were 2.34×10^2 and 1.12×10^3 M^{-1} s^{-1}, respectively, that is, 4.6-fold larger for PC1. Authors (*16*) have pointed out that the better PC1 radical stabilization may be due to the hyperconjugation between the π electrons on ring B and the σ electrons on the C2 atom in ring C deriving from its planarity.

On the other hand, it is well known (*17*) that factors such as conjugation and electron delocalization can contribute significantly to the stabilization of the radical form of antioxidants, improving their performance as scavengers. To rationalize experimental findings, we have undertaken a theoretical study concerning the antioxidant ability of catechin and its planar derivative PC1. We have determined the BDE and IP values and studied the mechanisms of the reaction of both catechin and PC1 molecules with $^\bullet$OOH hydroperoxyl radical.

MATERIALS AND METHODS

All of the calculations reported in this study were performed with the Gaussian03 code (*18*). The geometries of catechin and PC1 neutral molecules and their radicals, as well as that of $^\bullet$OOH and HOOH species, were optimized without constraints using the B3LYP (*19, 20*) exchange-correlation functional and the 6-311++G** basis set (*21, 22*). Vibrational frequencies were computed at the same level of theory, with the aim to characterize all structures as minima and saddle points and to estimate zero point energy corrections.

The unrestricted open-shell approach was used for radical species. No spin contamination was found for radicals, because the $<S^2>$ values were 0.750 in all cases. Intrinsic reaction coordinate (IRC) calculations (*23*) were performed at the same level of theory to confirm that a given transition state connects reactants and products.

Solvent effects were computed in the framework of self-consistent reaction field polarizable continuum model (SCRF-PCM) (*24–26*), using the UAHF (*27*) set of solvation radii to build the cavity for the solute, in the gas phase equilibrium geometries. The dielectric constants of 78.39 and of 36.64 were chosen to reproduce the water and acetonitrile (MeCN) media, respectively.

Natural bond orbital (NBO) analysis (*28*) implemented in the Gaussian03 package was used to characterize the electronic structures of the systems under investigation. The OH bond dissociation energy (BDE) and ionization potential (IP) values were computed at 298 K as the enthalpy difference for the H-atom and the one-electron transfer reactions.

RESULTS

BDE and IP evaluation. The equilibrium geometries of neutral catechin and PC1 are reported in **Figure 1**, together with the orbital composition of their highest occupied molecular orbitals (HOMOs). The catechin lowest energy structure (see figure **1**) is characterized by a torsional C2′–C1′–C2–C3 angle of 77.4° that indicates that rings B and C are almost mutually perpendicular. Hydroxyls in ring B are arranged as to establish an hydrogen bond whose length is 2.152 Å. The electronic delocalization occurs independently on rings B and A, as the values of bond order confirm (see Table S1 in the Supporting Information).

The same torsional dihedral in PC1 was found to be 156.0°, due to the formation of the six member ring in which the 3-OH group oxygen atom is involved (**Figure 1**). This torsion value indicates that a quite planar disposition of rings B and C is present. As in the catechin, also for PC1, the 3′- and 4′-OH groups are weakly linked by an H-bond (2.160 Å). π electrons are delocalized over the aromatic rings B and A. Bond order analysis (see Table S1) suggests that a single bond exists between the C2 and the C1′ atoms so that there is no possibility of conjugation between the rings B and C, as expected.

The different structural arrangements of the two systems are in full view in the HOMOs composition, reported in **Figure 1**. In catechin, the charge density is mainly localized on the aromatic ring A, with a lesser involvement of the chromane moiety. In PC1, the electron density is distributed in all rings, with a sensible increase on ring B, due to the nearly planar arrangement.

The abstraction of a hydrogen atom from each OH group present in the considered molecules gives rise to four radical species for both catechin and PC1. The relative energies of these radicals are collected in **Table 1**.

The most stable radical for catechin is the 4′-O$^\bullet$ (Figure S1 in Supporting Information), which arises from the removal of

Table 1. B3LYP/6-311++G** Relative Energies of Catechin and PC1 Radicals (Enthalpies Values in kcal/mol)

	catechin	PC1
3'-O$^\bullet$	0.7	0.0
4'-O$^\bullet$	0.0	0.0
5-O$^\bullet$	8.1	9.0
7-O$^\bullet$	7.9	8.9

the hydrogen atom from the OH group attached to the C4'-position. It is almost isoenergetic ($\Delta E = 0.7$ kcal/mol) with the 3'-O$^\bullet$ radical. Both forms retain the hydrogen bond existing before the radicalization process, although, in the 3'-O$^\bullet$ species, the H bond must be restored by a rotation of 180° around the C4'-OH axis. Part of the stability exhibited by 4'-O$^\bullet$ and 3'-O$^\bullet$ radicals can be attributed to the adjacent hydroxyls on ring B, as exhaustively pointed out elsewhere (*10–13*).

The other species are found at 8.1 (5-O$^\bullet$) and 7.9 (7-O$^\bullet$) kcal/mol above the absolute minimum (**Table 1**). Relative energies of these species indicate that the main factor contributing to the radical stability is the H-bond established between the adjacent hydroxyls (4'-O$^\bullet$ and 3'-O$^\bullet$ species).

PC1 radicals relative energies (**Table 1**) follow the same trend obtained for the nonplanar catechin, with the exception that now the 3'-O$^\bullet$ and 4'-O$^\bullet$ species are completely isoenergetic. The 5-O$^\bullet$ and 7-O$^\bullet$ radicals are found at 9.0 and 8.9 kcal/mol with respect to the 4'-O$^\bullet$/3'-O$^\bullet$ one.

Figure 2 illustrates the plot of the spin density distribution on the most stable radicals 4'-O$^\bullet$ of catechin and PC1. As can be noted, in catechin radical 4'-O$^\bullet$, the spin density is mainly localized on ring B. The H-bond between the remaining OH group and the radicalized oxygen confines the spin density on this site. In the case of PC1 4'-O$^\bullet$ radical, the odd electron is mainly found on the radicalization site and in a less extent on all atoms of ring B.

The cation radicals arising from the single electron abstraction in catechin and PC1 (see Figure S2 in the Supporting Information) are different as far as the delocalization of the odd electron is concerned and reflects the structure of the respective parent molecule HOMOs. In fact, in the catechin radical cation, the spin distribution (**Figure 3**) shows that the odd electron is confined on the oxygen atom belonging to the 5-OH group in ring A. For PC1, the spin density is localized mainly in ring B, but a certain degree of delocalization over the rings A and C is also present. **Table 2** lists the gas-phase and in water solution BDEs and the IPs (in kcal/mol) obtained for catechin and PC1.

The gas-phase BDE values for the 3'-OH, 4'-OH, 5-OH, and 7-OH groups of catechin are 74.9, 74.2, 82.3, and 82.1 kcal/mol, respectively. A lesser amount of energy is required for breaking the 3'-OH and 4'-OH group with respect to the 5-OH and 7-OH ones. This is not surprising if we consider that in the case of the 3'-OH and 4'-OH, the H$^\bullet$ abstraction produces the two most stable radicals.

In the case of PC1, absolute gas-phase BDE values for the 3'-OH and 4'-OH groups are smaller by 1 kcal/mol (73.3 kcal/mol) with respect to those of corresponding radicals of catechin. No significant difference between catechin and PC1 is found in the BDE values for 5-OH and 7-OH groups. This indicates that the planar configuration mainly affects the BDE for the hydroxyls on ring B, while no effect is obtained for the hydroxyls on ring A.

3'-OH and 4'-OH BDE values of the tautomers of catechin and PC1, in which the 4'-OH is the donor and the 3'-OH is the acceptor for the H-bond, were computed to be 75.1 and 74.4 and 73.7 and 73.8 kcal/mol for catechin and PC1, respectively

(see in **Table 2** the values in parentheses). So, the relative stabilities of the 3'-O$^\bullet$ and 4'-O$^\bullet$ radicals are not affected by the tautomerism of the H-bonding in ring B.

BDEs computed in the condensed phase are higher than those obtained in the gas phase by ≈9 kcal/mol. This can be ascribed to the minor stability of radical species in the water medium. However, 3'-OH and 4'-OH BDEs are smaller for PC1 than for catechin.

The IPs for catechin and PC1 were computed to be 169.7 and 166.8 kcal/mol in the gas phase, respectively. The difference of 2.9 kcal/mol can be considered as a measure of the stability arising from the planar arrangement of PC1.

The values in water solution are of 135.7 and 136.0 kcal/mol for catechin and PC1, respectively. They underline that the electron transfer process is favored by the medium. However, because the PC1 molecule is less polar than catechin, the IPs are almost the same. On the basis of obtained results, one can conclude that the geometry obtained by constraining ring B and the chromane moiety to be coplanar affects mainly the IP value.

Reaction with $^\bullet$OOH: Comparison among Catechin, PC1, and Quercetin. The results obtained for BDE and IP of catechin and PC1 have shown that the planar arrangement of the second molecule has a slight effect on both these quantities. Thus, as indicated by experimental findings (*16*) in the case of the reaction of these two antioxidants with the galvinoxyl radical, the PC1 should improve the inactivation process of radicals, making it faster than that involving nonplanar catechin.

To verify the experimental findings, we have determined the potential energy surface (PES) for the hydrogen abstraction from catechin and PC1 by $^\bullet$OOH radical, in gas phase and in MeCN. On the basis of the indication derived from the first part of this work, only the 4'-OH most favorite radicalization site has been considered for both molecules. The $^\bullet$OOH radical has been chosen as a prototype of oxygen-centered radical species. The PESs for catechin (solid line) and PC1 (dashed line) are reported in **Figure 4**. The equilibrium geometries of the stationary points along the PESs are reported in Figure S3 in the Supporting Information.

The reaction begins with the formation of a complex between the catechin and the $^\bullet$OOH radical that attaches the 4'-OH group in the flavanol molecule. A hydrogen bond is established between them, whose length is computed to be 1.950 Å. The dihedral C2'–C1'–C2–C3 does not undergo modification on the interaction with the hydroperoxide (76.4°). The H-bond between the 3'-OH (donor) and the 4'-OH (acceptor) is retained in going from separated to interacting reactants. The formation of the complex is exothermic by 5.4 kcal/mol.

The transition state for the abstraction of the H$^\bullet$ by the hydroperoxide radical is located at 0.1 kcal/mol above the reactants asymptote and is characterized by 4'OH–OOH and 4'O–HOOH distances of 1.286 and 1.113 Å, respectively. The imaginary frequency at 1454 cm^{-1} corresponds to the stretching of these bonds. The activation energy required to overcome this saddle point is 5.5 kcal/mol, so that the reaction with the hydroperoxide radical is very fast.

After the TS, a weak bond complex between the radicalized catechin and the HOOH is found lying 16.7 kcal/mol below the reactants. The distance between the C4'-O$^\bullet$ radicalized oxygen and the H-OOH hydrogen is 1.807 Å. Products, catechin 4'-O$^\bullet$ radical and HOOH, are found 8.4 kcal/mol below the reference and obtained in a barrierless process.

The formation of the complex between the PC1 molecule and the $^\bullet$OOH radical is exothermic by 5.3 kcal/mol, so that no

Antioxidant Power of Flavonoid Catechin

J. Agric. Food Chem., Vol. 55, No. 19, 2007 **7947**
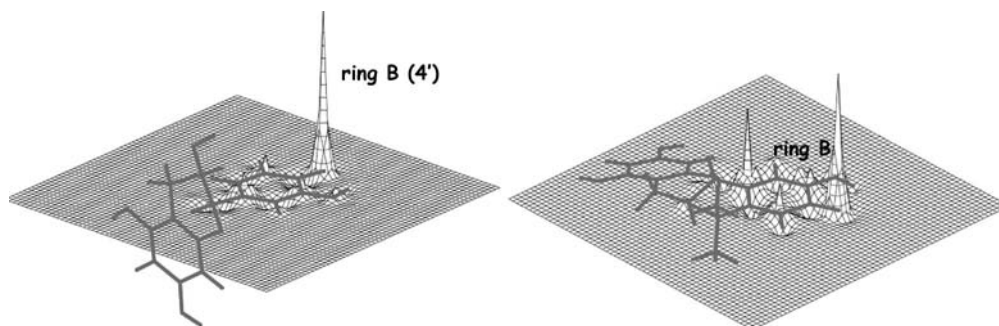

Figure 2. Spin distribution of the 4′-O• radicals of catechin (left) and PC1 (right).
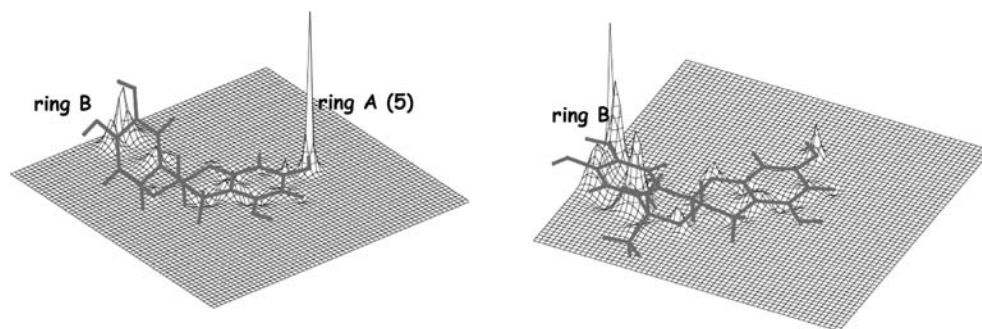

Figure 3. Spin distribution of the radical cations of catechin (left) and PC1 (right).

Table 2. B3LYP/6-311++G** Gas-Phase and in Water BDEs and IPs of Catechin and PC1 (Enthalpies Values in kcal/mol)

	catechin	PC1	catechin	PC1
	BDE (gas)		BDE (water)	
3′-OH	74.9 (75.1)	73.3 (73.7)	83.5	82.0
4′-OH	74.2 (74.4)	73.3 (73.8)	83.0	82.2
5-OH	82.3	82.3	88.8	88.8
7-OH	82.1	82.2	88.4	88.4
	IP (gas)		IP (water)	
	169.7	166.8	135.7	136.0

effect due to the planar disposition is obtained in the formation of the reactants complex. Also, in PC1, a hydrogen bond is established between the hydroperoxide radical and the 4′-OH group (1.936 Å).

In the transition state that lies 0.9 kcal/mol below the reactants, the bonds 4′OH–OOH and 4′-O–HOOH measure 1.305 and 1.102 Å, respectively. The vibrational normal mode with an imaginary frequency of 1324 cm^{-1} is characterized by the stretching of this couple of bonds. The activation energy is 4.4 kcal/mol, that is, 1.1 kcal/mol lower than that computed for the nonplanar catechin.

The complex between the PC1 4′-O• radical and the neutral HOOH species shows a relative energy (with respect to the reactants) of −18.3 kcal/mol. The fact that this complex is significantly more stable than products (by 9.0 kcal/mol) is usually recognized as a positive effect for the antioxidant ability (*29*). In fact, the H$_2$O$_2$ still bound to the antioxidant radical after the hydrogen abstraction should prevent the possibility that both of these species can attack on lipids in the membrane.

In the work of Fukuhara (*16*), the rate constant for quercetin was also determined and its value was found to be approximately the same of the one obtained for PC1. For reason of comparison, the gas-phase hydrogen abstraction PES from quercetin by •OOH radical was also determined. The quercetin behavior is very similar to that of PC1. The formation of the reactants complex is exothermic by 5.3 kcal/mol. The transition state (imaginary frequency at 1489 cm^{-1}) is located 0.8 kcal/mol below the
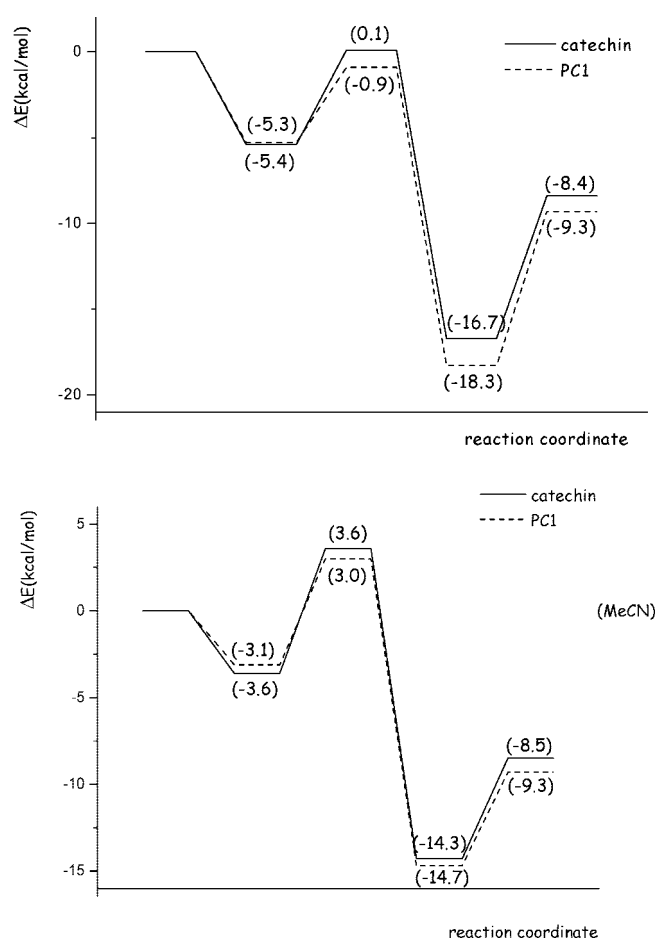

Figure 4. Potential energy surfaces for the reaction of hydroperoxide with catechin (solid line) and PC1 (dashed line), in vacuo (top) and in acetonitrile medium (bottom).

reference. The activation energy is computed to be 4.5 kcal/mol, that is, practically the same obtained for PC1 (4.4 kcal/

mol). The products complex and the products are found 16.6 and 9.3 kcal/mol below the reference, respectively.

Computations in the acetonitrile medium do not introduce meaningful differences with respect to the gas-phase ones. The formation of reactants complex is less exothermic for both catechin (3.6 kcal/mol) and PC1 (3.1 kcal/mol). The transition state for ˙H abstraction by ˙OOH is found at 3.6 and 3.0 kcal/mol for catechin and PC1, respectively. The corresponding activation energies of 7.2 and 6.1 kcal/mol indicate that ˙H removal is less favored in the condensed phase than in vacuo. The weak complex between products and the products are found 14.3 and 8.5 and 14.7 and 9.3 kcal/mol, below the reference for catechin and PC1, in that order.

Recently, the activation barriers for the reactions between tocopherol and ˙OOH radical were determined. (*29*) The activation energy for the H˙ abstraction from the only OH was computed to be 8.8 kcal/mol, which is greater that those computed here for catechin, PC1, and quercetin. This finding reinforces the stabilizing effect of the internal hydrogen bond between adjacent hydroxyls on the transition state.

From the comparison of the PESs in **Figure 4**, some comments on the antioxidant power of catechin and its planar analogue can be done. The reactants complex formation is not affected by the planar arrangement, because the binding energy is practically the same in both situations. The activation energy is lower for PC1 than for catechin by 1.1 kcal/mol. The formation of the weak bond complex between products is thermodynamically more favored for planar catechin, because it is located 18.3 kcal/mol below the reference, while for catechin, it is found to be 16.7 kcal/mol below the corresponding reference. So, the abstraction reaction in the case of PC1 is also favored thermodynamically.

A further indication about the reaction rates for catechin and PC1 can be derived based on the Arrhenius formula, $k = k_B T/h \times e^{-\Delta G/RT}$, where k_B is the Boltzmann's constant, T is the absolute temperature, h is the Planck constant, ΔG is the difference in Gibbs free energy between TS and reactants, and R is the constant of gas.

Although theoretical calculations cannot be used to obtain accurate rate constants, because an error of only few kcal/mol in the barrier evaluation, even if normally allowed in the calculations, corresponds to an error of several orders of magnitude in the rate; nevertheless, it is possible to estimate the ratio between computed rate constants since in this case the error can be mutually cancelled.

The k_{PC1}/k_{cat} ratio was found to be 3.9, which means that the abstraction reaction is ≈4-fold faster with PC1 rather than with catechin. With the same procedure, the ratio k_{PC1}/k_{que} was evaluated approximately to be equal to 1, so that one can conclude that planar catechin and quercetin show similar kinetics. By taking into account the methodological limits, the agreement with the experimental indications is quite satisfactory being the measured k_{PC1}/k_{cat} and k_{PC1}/k_{que} ratios 4.6 and 0.96, respectively (*16*).

Conclusions. The antioxidant activity of the flavonol catechin and one of its planar analogue, PC1, has been investigated theoretically computing the OH BDE and the IP values and by determining the potential energy surface for the H˙ abstraction reaction from the phenolic hydrogen by the ˙OOH radical. The aim of the work was to verify if the planar geometry may affect the antioxidant power of catechin. The values of BDEs indicate that both molecules can act through the hydrogen atom transfer mechanism because 74.2 and 73.3 kcal/mol are required to break the OH bond in catechin and PC1, respectively. The planar

arrangement seems to affect slightly the electronic features of the phenolic OH bond that must be broken during the H˙ abstraction.

In the case of the electron transfer mechanism instead, the planar configuration quite affects the features of the HOMO and lowers the energy required for the removal of the single electron, as the gas-phase values of 169.7 and 166.8 kcal/mol in the IPs, for catechin and PC1, respectively, show. The study of the kinetics of the antioxidant process occurring through the reaction with the hydroperoxy radical points out that the reaction is kinetically favored by the planar disposition because the barrier height for the hydrogen abstraction is lower for the PC1 by 1.1 kcal/mol. Estimation of the rate constants for both molecules indicates that these differences in the activation barriers make the reaction involving PC1 4-fold faster with respect to catechin, remarking the experimental indications. The relative energy of the reaction products indicates that the hydrogen abstraction in the presence of the planar catechin is also favored thermodynamically.

Supporting Information Available: Table containing bond order values for catechin, planar catechin 1 (PC1), and their radicals. Figures containing minimum energy geometries of most stable radicals of catechin and PC1. Figure containing the stationary points along the potential energy surface for the reaction of catechin and PC1 with hydroperoxide radical. This material is available free of charge via the Internet at http://pubs.acs.org.

LITERATURE CITED

(1) Hsieh, R. J.; Kinsella, J. E. Oxidation of polyunsaturated fatty acids: Mechanisms, products, and inhibition with emphasis on fish. *Adv. Food Nutr. Res.* **1989**, *33*, 233–341.

(2) Ko, F.; Chu, C.; Lin, C.; Chang, C.; Teng, C. Isoorientin-6-O-glucoside, a water-soluble antioxidant isolated from *Gentiana arisanensis*. *Biochem. Biophys. Acta* **1998**, *1389*, 81–90.

(3) Novic, M.; Nikolovska, Z.; Solmajer, T. Quantitative structure-activity relationship of flavonoid p56[lck] protein tyrosine kinase inhibitors. A neural network approach. *J. Chem. Inf. Comput. Sci.* **1997**, *37*, 990–998.

(4) Amic, D.; Davidovic, D.; Juric, A.; Lucic, B.; Trinajstic, N. Structure-activity correlation of flavone derivatives for inhibition of cAMP phosphodiesterase. *J. Chem. Inf. Comput. Sci.* **1995**, *35*, 1034–1038.

(5) Uda, Y.; Price, K.; Williamson, G.; Rhodes, M. Induction of the anticarcinogenic marker enzyme, quinone reductase, in murine hepatoma cells in vitro by flavonoids. *Cancer Lett.* **1997**, *120*, 213–216.

(6) Tahara, S.; Katagiri, Y.; Ingham, J.; Mizutani, J. Prenylated flavonoids in the root of yellow lupin. *Phytochemistry* **1994**, *36*, 1261–1271.

(7) Amoros, M.; Simoes, C. M. O.; Girre, L.; Sauvager, F.; Cormier, M. Synergistic effect of flavones and flavonols against herpes simplex virus type 1 in cell culture. Comparison with the antiviral activity of propolis. *J. Nat. Prod.* **1992**, *55*, 1732–1740.

(8) Visioli, F.; Bellomo, G.; Galli, C. Free radical-scavenging properties of olive oil polyphenols. *Biochem. Biophys. Res. Commun.* **1998**, *247*, 60–64.

(9) Visioli, F.; Galli, C. Olive oil polyphenols and their potential effects on human health. *J. Agric. Food Chem.* **1998**, *46*, 4292–4296.

Antioxidant Power of Flavonoid Catechin

J. Agric. Food Chem., Vol. 55, No. 19, 2007 **7949**

(10) Wright, J. S.; Johnson, E. R.; Di Labio, G. A. Predicting the activity of phenolic antioxidants: Theoretical method, analysis of substituent effects and application to major families of antioxidants. *J. Am. Chem. Soc.* **2001**, *123*, 1173–1183.

(11) Leopoldini, M.; Prieto Pitarch, I.; Russo, N.; Toscano, M. Structure, conformation and electronic properties of apigenin, luteolin and taxifolin antioxidants. A first principle theoretical study. *J. Phys. Chem. B* **2004**, *108*, 92–94.

(12) Leopoldini, M.; Marino, T.; Russo, N.; Toscano, M. Antioxidant properties of phenolic compounds. H-atom versus electron transfer mechanism. *J. Phys. Chem. B* **2004**, *108*, 4916–4922.

(13) Leopoldini, M.; Marino, T.; Russo, N.; Toscano, M. Density functional computations of the energetic and spectroscopic parameters of quercetin and its radicals in the gas phase and in solvent. *Theor. Chem. Acc.* **2004**, *111*, 210–216.

(14) Manach, C.; Scalbert, A.; Morand, C.; Remesy, C.; Jimenez, L. Polyphenols: Food sources and bioavailability. *Am. J. Clin. Nutr.* **2004**, *79*, 727–747.

(15) Hakamata, W.; Nakanishi, I.; Masuda, Y.; Shimizu, T.; Higuchi, H.; Nakamura, Y.; Saito, S.; Urano, S.; Oku, T.; Ozawa, T.; Ikota, N.; Miyata, N.; Okuda, H.; Fukuhara, K. Planar catechin analogues with alkyl side chains: A potent antioxidant and an χ-glucosidase inhibitor. *J. Am. Chem. Soc.* **2006**, *128*, 6524–6525.

(16) Fukuhara, K.; Nakanishi, I.; Kansui, H.; Sugiyama, E.; Kimura, M.; Shimada, T.; Urano, S.; Yamaguchi, K.; Miyata, N. Enhanced radical-scavenging activity of a planar catechin analogue. *J. Am. Chem. Soc.* **2002**, *124*, 5952–5953.

(17) Rice-Evans, C. A.; Miller, J. N.; Paganga, G. Structure-antioxidant activity relationships of flavonoids and phenolic acids. *Free Radical Biol. Med.* **1996**, *20*, 933–956.

(18) Frisch, M. J.; Trucks, G. W.; Schlegel, H. B.; Scuseria, G. E.; Robb, M. A.; Cheeseman, J. R.; Montgomery, J. A., Jr.; Vreven, T.; Kudin, K. N.; Burant, J. C.; Millam, J. M.; Iyengar, S. S.; Tomasi, J.; Barone, V.; Mennucci, B.; Cossi, M.; Scalmani, G.; Rega, N.; Petersson, G. A.; Nakatsuji, H.; Hada, M.; Ehara, M.; Toyota, K.; Fukuda, R.; Hasegawa, J.; Ishida, M.; Nakajima, T.; Honda, Y.; Kitao, O.; Nakai, H.; Klene, M.; Li, X. ; Knox, J. E.; Hratchian, H. P.; Cross, J. B.; Adamo, C.; Jaramillo, J.; Gomperts, R. S.; Stratmann, R. E.; Yazyev, O.; Austin, A. J.; Cammi, R.; Pomelli, C.; Ochterski, J. W.; Ayala, P. Y.; Morokuma, K.; Voth, G. A.; Salvador, P.; Dannenberg, J. J.; Zakrzewski, V. G.; Dapprich, S.; Daniels, A. D.; Strain, M. C.; Farkas, O.; Malick, D. K.; Rabuck, A. D.; Raghavachari, K.; Foresman, J. B.; Ortiz, J. V.; Cui, Q.; Baboul, A. G.; Clifford, S.; Cioslowski, J. ; Stefanov, B. B.; Liu, G.; Liashenko, A.; Piskorz, P.; Komaromi, I.; Martin, R. L.; Fox, D. J.; Keith, T.; Al-Laham, M. A.; Peng, C. Y.; Nanayakkara, A.; Challacombe, M.; Gill, P. M. W.; Johnson, B.; Chen, W.; Wong, M. W.; Gonzalez, C.; Pople, J. A. *Gaussian*; Gaussian Inc.: Pittsburgh, PA, 2003.

(19) Becke, A. D. J. Density-functional thermochemistry. 3. The role of exact exchange. *Chem. Phys.* **1993**, *98*, 5648–5652.

(20) Lee, C.; Yang, W.; Parr, R. G. Development of the Colle-Salvetti correlation-energy formula into a functional of the electron density. *Phys. Rev. B* **1988**, *37*, 785–789.

(21) Ditchfield, R.; Hehre, W. J.; Pople, J. A. Self-consistent molecular-orbital methods: IX. An extended Gaussian-type basis for molecular-orbital studies of organic molecules. *J. Chem. Phys.* **1971**, *54*, 724–728.

(22) Hehre, W. J.; Ditchfield, R.; Pople, J. A. Self-consistent molecular orbital methods: XII. Further extensions of Gaussian-type basis sets for use in molecular orbital studies of organic molecules. *J. Chem. Phys.* **1972**, *56*, 2257–2261.

(23) Gonzalez, C.; Schlegel, H. B. An improved algorithm for reaction path following. *J. Chem. Phys.* **1989**, *90*, 2154–2161.

(24) Miertus, S.; Scrocco, E.; Tomasi, J. Electrostatic interaction of a solute with a continuum. A direct utilization of ab initio molecular potentials for the prevision of solvent effects. *Chem. Phys.* **1981**, *55*, 117–129.

(25) Miertus, S.; Tomasi, J. Approximate evaluations of the electrostatic free energy and internal energy changes in solution processes. *Chem. Phys.* **1982**, *65*, 239–245.

(26) Cossi, M.; Barone, V.; Cammi, R.; Tomasi, J. Ab initio study of solvated molecules: a new implementation of the polarizable continuum model. *Chem. Phys. Lett.* **1996**, *255*, 327–335.

(27) Barone, V.; Cossi, M.; Tomasi, J. A new definition of cavities for the computation of solvation free energies by the polarizable continuum model. *J. Chem. Phys.* **1997**, *107*, 3210–3221.

(28) Carpenter, J. E.; Weinhold, F. Analysis of the geometry of the hydroxymethyl radical by the different hybrids for different spins natural bond orbital procedure. *J. Mol. Struct. (Theochem)* **1988**, *169*, 41–62.

(29) Navarrete, M.; Rangel, C.; Espinosa-Garcia, J.; Corchado, J. C. Theoretical study of the antioxidant activity of vitamin E: Reactions of tocopherol with the hydroperoxy radical. *J. Chem. Theor. Comp.* **2005**, *1*, 337–344.